

Linear Constraints Learning for Spiking Neurons

Huy Le Nguyen*, Dominique Chu

CEMS, School of Computing, University of Kent, Canterbury, CT2 7NF, UK

Abstract

We introduce a new supervised learning algorithm based to train spiking neural networks for classification. The algorithm overcomes a limitation of existing multi-spike learning methods: it solves the problem of interference between interacting output spikes during a learning trial. This problem of learning interference causes learning performance in existing approaches to decrease as the number of output spikes increases, and represents an important limitation in existing multi-spike learning approaches. We address learning interference by introducing a novel mechanism to balance the magnitudes of weight adjustments during learning, which in theory allows every spike to simultaneously converge to their desired timings. Our results indicate that our method achieves significantly higher memory capacity and faster convergence compared to existing approaches for multi-spike classification. In the ubiquitous Iris and MNIST datasets, our algorithm achieves competitive predictive performance with state-of-the-art approaches.

Keywords: Spiking neural networks, Multi-spike learning, Constraint optimization, Supervised learning, Classification

1. Introduction

Spiking Neural Networks (SNNs) are a type of neural networks (Gerstner and Kistler, 2002) that is more biologically plausible compared to the traditional Artificial Neural Networks (ANNs) (Prieto et al., 2016) commonly used in deep learning. In SNNs, a neuron processes and transmits information to others via sequences of discrete events called spikes. This information can typically be encoded in the frequency (rate-coding) or the precise spike timings (temporal coding) of the spike sequences (Van Rullen and Thorpe, 2001). In contrast, the output

*Corresponding author. Email address: hln7@kent.ac.uk

of sigmoidal neurons used in ANNs represents continuous spiking frequencies, and so the operation of such neurons is limited to rate-coding. SNNs with temporal coding have been shown to be more computationally powerful than ANNs (Maass, 1997), even on the level of single neurons (Rubin et al., 2010). Furthermore, it has been shown that allowing spiking neurons to generate multiple spikes can increase the diversity, richness, and capacity of information representation in temporal coding schemes (Borst and Theunissen, 1999; Xu et al., 2013; Ponulak and Kasiński, 2010). Therefore, much research into supervised learning for SNNs have focused on developing efficient multi-spike learning algorithms. (Ponulak and Kasiński, 2010; Yu et al., 2013; Gardner and Grüning, 2016; Taherkhani et al., 2018; Xiao et al., 2019; Gardner and Grüning, 2021).

One of the main difficulties with multi-spike learning is the problem of learning interference. When learning to generate multiple desired output spikes, updating weights to adjust the timing of one output spike changes the timing of this spike, but inevitably also the timings of other spikes Xu et al. (2013); Gardner and Grüning (2016). We will present experimental evidence which suggests that even in the simple case of two output spikes, this learning interference is detrimental to training efficiency (requiring up to ten times more training epochs), or causes non-convergence (weights diverging from their optimal values). A solution to the learning interference problem has not been proposed Taherkhani et al. (2020), and affected learning algorithms either demonstrate relatively low capacity to memorise (fit) training data (Ponulak, 2005; Florian, 2012; Mohemmed et al., 2012; Yu et al., 2013; Gardner and Grüning, 2016), or achieve high memory capacity but converges slowly (Memmesheimer et al., 2014). For example, the Finite-Precision (FP) algorithm suggested in Memmesheimer et al. (2014) trains SNNs to correctly respond to a large number of inputs, but requires fifty million training epochs for convergence. Another example is the PSD algorithm suggested in Yu et al. (2013), which reliably converges in under five hundred epochs, but demonstrates much lower memory capacity compared to the FP algorithm.

In this paper, we propose a new supervised learning algorithm for training single-layer SNNs to perform classification with multiple spikes, which achieves both high memory capacity and fast convergence. We call this the *Discrete Threshold Assumption* (DTA) algorithm. In precise input-output mapping tasks, our algorithm achieves approximately twice the maximal memory capacity compared to the PSD (Yu et al., 2013) and FILT algorithms (Gardner and Grüning, 2016), and converges in several orders of magnitude fewer epochs compared to the FP and HTP algorithms (Memmesheimer et al., 2014). In Tempotron learning tasks (Gütig and Sompolinsky, 2006; Gutig, 2016), our method achieves three times the

memory capacity and ten times faster convergence compared to the seminal MST algorithm (Gutig, 2016). In the practical setting, our algorithm demonstrates competitive accuracy and convergence speed to state-of-the-art methods on Fisher’s Iris dataset (Fisher, 1936) and the popular MNIST dataset (LeCun and Cortes, 2010).

Our method demonstrates that the problem of learning interference in multi-spike learning can be solved for single-layer SNNs, and thus show that learning efficiency does not have to decrease as the number of output spikes increases (Xu et al., 2013). Our method achieves this by employing a novel mechanism during learning, which takes the form of a global supervisory signal designed to ‘balance’ the magnitude of weight updates with respect to each output spike time. We formulate this supervisory signal as a linear constraint satisfaction problem, and the basic idea is to compute the temporal correlations between output spike timings. Weight adjustments can then be made such that the effects of learning interference are compensated for, and so already converged spikes are not affected by weight adjustment. In theory, this allows every output spike to converge to their desired timings simultaneously. In practice, the continuous nature of the temporal dimension in the neuron model is problematic, and convergence still requires a number of training iterations.

The rest of the paper is organised as follows. In Section 2.1, we describe the neuron model, as well as the definitions of spiking input and output sequences. In Section 2.2, the supervised learning tasks and their notations are introduced. In Section 2.3, the learning interference problem is defined and illustrated by a simple learning scenario. In Section 2.4, we describe the DTA algorithm in detail. In Section 2.5, we evaluate and analyse the memory capacity of our algorithm, compared to various methods in the literature. In Section 2.6, we evaluate the generalisation performance of our algorithm in practical settings by applying the algorithm to the IRIS and MNIST datasets. Finally, in Section 3 we discuss the DTA algorithm in the context of the wider literature, specifically regarding potential avenues to extend our method to train multi-layer SNNs.

2. Results

In this section, we will first introduce the neuron model and the spike-based classification tasks. Then, we will describe the proposed DTA algorithm and how it solves the problem of learning interference for multi-spike problems.

2.1. Neuron Model

We consider the simplified Spike Response Model (SRM) for its computational simplicity and analytical tractability (Gerstner and Kistler, 2002). The model consists of $N \in \mathbb{N}^+$ weighted input channels, an output channel, and an internal state that changes over time. Input spikes to a neuron affect the real-valued internal state $V(t)$ of the neuron (called membrane potential) over time. When $V(t)$ crosses a constant threshold value ϑ from below, the neuron generates an output spike modelled as the Dirac Delta function $\delta(t)$. An input spike arriving at an input channel at time $t^i \in \mathbb{R}^+$ is modelled as $\delta(t - t^i)$, and an output spike generated by the neuron to its output channel at time $t^o \in \mathbb{R}^+$ is modelled as $\delta(t - t^o)$.

We denote the set of input spikes to input channel i as $x_i = \{t_1^i, t_2^i, t_3^i, \dots\}$. An *input pattern* is defined here as a vector containing specific spike sequences to each input channel, denoted as $\mathbf{x} = \{x_1, x_2, \dots, x_N\}$. The set of output spike times generated by the neuron is denoted as $o(\vartheta, \mathbf{x}, w) = \{t_1^o, t_2^o, t_3^o, \dots\}$. Unless stated otherwise, input patterns \mathbf{x} are randomly generated and fixed. When the training data is composed of $P \geq 1$ input patterns, the patterns are denoted \mathbf{x}_p . Each input spike in a spike sequence x_i is generated using a homogenous Poisson point process with rate ν_{in} and maximum time value $T \in \mathbb{R}^+$. One of the learning tasks we will consider in this paper requires specifying a desired output spike sequence for each input pattern, the timings of which are generated similarly with rate ν_{out} .

The momentary membrane potential $V(t)$ of the neuron is defined by the following equations:

$$V(t) = \sum_{i=1}^N w_i \sum_{t^i \in x_i} \lambda(t - t^i) - \vartheta \sum_{t^o \in o(\vartheta, \mathbf{x}, w)} \gamma(t - t^o) \quad (1)$$

$$\lambda(t - t^i) = V_{\text{norm}} \left(\exp \left(\frac{-(t - t^i)}{\tau_m} \right) - \exp \left(\frac{-(t - t^i)}{\tau_s} \right) \right) \Theta(t - t^i) \quad (2)$$

$$\gamma(t - t^o) = \exp \left(-\frac{t - t^o}{\tau_m} \right) \Theta(t - t^o) \quad (3)$$

Here, τ_m and τ_s are time constants of the membrane potential and synaptic currents, respectively. The constant V_{norm} normalises the peak value of function $\lambda(t)$ to 1:

$$\xi = \frac{\tau_m}{\tau_s}$$

$$V_{\text{norm}} = \frac{\xi^{\frac{\xi}{\xi-1}}}{\xi - 1}$$

And the Heaviside step function:

$$\Theta(t) = \begin{cases} 1, & \text{if } t \geq 0 \\ 0, & \text{otherwise} \end{cases}$$

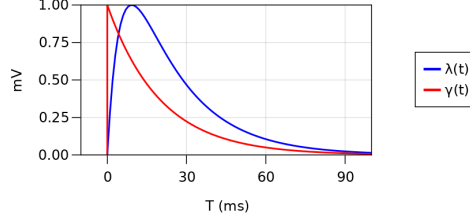


Figure 1: The shapes of the PSP kernel λ and the reset kernel γ in the neuron model, with $\tau_m = 20.0$ and $\tau_s = 5.0$.

The post-synaptic potential (PSP) function $\lambda(t)$ converts each input spike time into an analog membrane potential contribution that varies over time. The reset function $\gamma(t)$ describes the non-linear reset effect of a previous output spike on $V(t)$. The temporal shapes of $\lambda(t)$ and $\gamma(t)$ are illustrated in Figure 1.

2.2. Definition of Learning Tasks

This work will focus on solving multi-spike classification tasks using SNNs with a single trainable layer of spiking neurons. This means the SNN should discriminate fixed input patterns into a number of classes. In traditional ANNs, class predictions are typically decided by the output neuron with the largest (real-valued) output value. Since SNNs do not have real-valued outputs, classification must be decided by some method of output spike encoding, to translate output timings to meaningful class predictions. We will consider two of the most common approaches for classification with multiple spikes.

In the first method, the supervisory signal provides a specific sequence of desired output spike timings for each input class. This means a trained SNN should

respond to an input pattern with spikes at the timings which correspond with the correct class. Classification is decided by the neuron with the most similar output response to the desired sequence, and so requires the calculation of some spike-based similarity measure (we use the Van Rossum metric (Rossum, 2001), see Appendix A). Gütiĝ (2014) calls this the *Encoding* task, because the network learns to produce mappings between input and output spike sequences. More formally, in the Encoding task the network is given P fixed input patterns \mathbf{x}_p and corresponding desired output sequences $y_p = \{t_1^d, t_2^d, t_3^d, \dots\}$, and we need to find weights w such that $o(\vartheta, \mathbf{x}_p, w) = y_p$ for $p = \{1, 2, \dots, P\}$. The Encoding task can be thought of as defining the following constraints on the membrane potential:

$$\begin{aligned} \vartheta &= V(t) \text{ at all spike times } t \in y_p && \text{(Threshold Equality)} \\ \vartheta &> V(t) \text{ at all other times } t \notin y_p && \text{(Threshold Inequality)} \end{aligned}$$

In the second method, the supervisory signal provides a number of desired output spikes for each input class, but no spike timings. As such, the important quantity is the number of output spikes, and these spikes may occur at any time. Gütiĝ (2014) calls this the *Decoding* task, as the classification can be directly decided by the number of output spikes, without any additional calculations. More formally, in the Decoding task the network is given P fixed input patterns \mathbf{x}_p and corresponding labels which define the desired number of output spikes for each pattern $l_p \in \mathbb{N}^+$. Solving this task entails finding weights w such that $|o(\vartheta, \mathbf{x}_p, w)| = l_p$ for $p = \{1, 2, \dots, P\}$, where $|m|$ denotes the cardinality of the set m .

The Decoding Task can be thought of as an Encoding task with unknown desired spike timings. It follows that in addition to learning to generate the desired spikes, the learning must also find appropriate timings when the spikes should occur. This process has advantages compared to the Encoding task. Specifically, the desired timings in the Encoding task are typically chosen without any specific reason (Bohte et al., 2002; Booiĝ and tat Nguyen, 2005; Ghosh-Dastidar and Adeli, 2009), and so it is difficult to determine whether the desired timings are optimal, such that solutions may exist for one selection of desired timings but not another. In the Decoding task, the freedom to choose output spike timings allows the learning process to identify meaningful input features regardless of when they occur, instead of only those which are temporally close to arbitrarily specified timings.

2.3. Learning Interference

A problem that one encounters when training SNNs to generate multiple output spikes ($l_p > 0$ for Encoding and $|y_p| > 0$ for Decoding) is a phenomenon

called ‘learning interference’ (Xu et al., 2013; Taherkhani et al., 2020). In this section, we will show that learning interference is an important limiting factor for the efficiency of multi-spike learning. We will develop an intuition for learning interference by first considering a first-error weight adjustment approach similar to the FP algorithm suggested by Memmesheimer et al. (2014). Then, we demonstrate the effects of learning interference in more detail with experimental data, which illustrates the effects of learning interference even in the simple scenario of learning to generate two output spikes.

For simplicity, we assume the learning task is Encoding. A training algorithm has to adjust neuron weights such that the threshold equality and inequality constraints (as described in the previous section) are satisfied. In continuous time, it is impossible to analytically satisfy an infinite number of threshold inequality constraints, so at each learning iteration we will only consider inequalities at the output spike times that have not converged to desired times. It then follows that there are two ways these constraints can be violated:

1. $\vartheta > V(t^d)$, for desired times $t^d \in y_p$
2. $\vartheta = V(t^o)$, for actual times $t^o \notin y_p$

Since \mathbf{x}_p and ϑ are fixed, the only variables that can be adjusted to modify $V(t)$ are the neuron weights. It is evident that we should increase weights contributing to $V(t^d)$ in type (1) violations, to increase $V(t^d)$ to ϑ . Similarly, we should decrease weights contributing to $V(t^o)$ in type (2) violations. These positive and negative weight adjustments can be respectively written as (Gütig and Sompolsky, 2006; Memmesheimer et al., 2014):

$$\begin{aligned}\Delta w_i^{\text{LTP}}(t^d) &= \eta \sum_{t^i \in x_i} \kappa(t^d - t^i) \\ \Delta w_i^{\text{LTD}}(t^o) &= -\eta \sum_{t^i \in x_i} \kappa(t^o - t^i)\end{aligned}\tag{4}$$

Here, η is a real-valued learning rate parameter, and $\kappa(t)$ is a temporal learning window which defines the magnitude of Δw_i as a function of the input information which is temporally local to the time of constraint violation t . In the remainder of this work, we will consider three different $\kappa(t)$ which are commonly used in the literature (Yu et al., 2013; Gardner and Grüning, 2016):

$$\kappa_{\text{STDP}}(t) = \exp\left(\frac{-t}{\tau_m}\right) \Theta(t) \quad (5)$$

$$\kappa_{\text{PSP}}(t) = \lambda(t) \quad (6)$$

$$\kappa_{\text{FILT}}(t) = \begin{cases} V_{\text{norm}} \left(C_m \exp\left(\frac{-t}{\tau_m}\right) - C_s \exp\left(\frac{-t}{\tau_s}\right) \right), & \text{if } t > 0 \\ V_{\text{norm}} (C_m - C_s) \exp\left(\frac{t}{\tau_m}\right), & \text{otherwise} \end{cases} \quad (7)$$

$$C_m = \frac{\tau_m}{\tau_m + \tau_s}$$

$$C_s = \frac{\tau_s}{\tau_m + \tau_s}$$

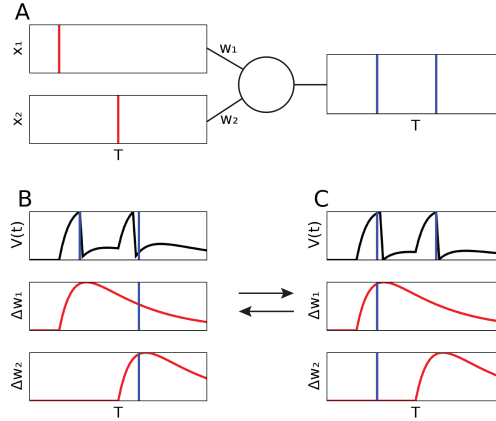


Figure 2: Illustration of learning interference with the first-error weight adjustment approach. **A:** the Encoding problem with two input spikes (red lines) and two desired output spikes (blue lines). **B:** (top) First spike is converged, second spike is earlier than desired. Hence, Δw_i^{LTD} is applied which changes both weights; (bottom) intersection between red and blue lines is $\kappa_{\text{PSP}}(t^d)$ for each weight. **C:** because of the previous weight update, the second spike is converged but the first is now later than desired. Adjusting the first spike with Δw_i^{LTP} then affects the second spike.

The first-error approach is to apply either Δw_i^{LTP} or Δw_i^{LTD} as appropriate to only the earliest constraint violation. We now apply this approach to a ‘toy’ problem (shown in Figure 2A), which involves a neuron with two input channels, each receiving one input spike at different timings to each other, and the two desired output spikes should occur shortly after each input spike. Learning interference is defined as the weight adjustment to move one output spike towards its desired

timing, having the unintended result of moving other spikes away from their desired timings. This concept is most simply illustrated when one output spike is already converged to the desired time (Figure 2B-C): adjusting the unconverged spike changes the timing of the already converged spike, which then requires re-learning the affected spike. This then affects the originally adjusted spike. In this manner, both weights oscillate around their optimal values, rather than smoothly converging to them.

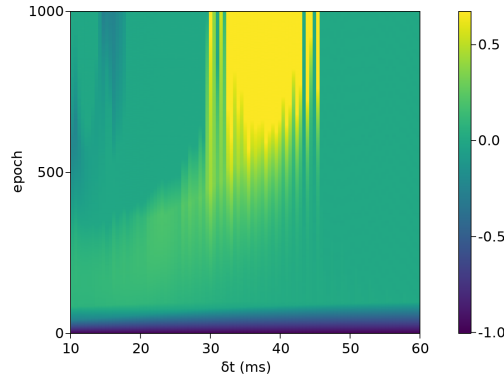


Figure 3: Effects of learning interference on the first neuron weight over the course of training. Vertical axis shows the training epoch. Horizontal axis shows the distance between the two desired output spikes (denoted δt). Colorbar shows the distance between the weight and its optimal value (0.0 is converged). At $\delta t > 50$ no learning interference is visible and the observed weight converges quickly. Otherwise, three effects of learning interference can be observed: at $\delta t < 20$ the weight fluctuates around the optimal value, $20 < \delta t < 30$ eventually converges after many training iterations, and $30 < \delta t < 40$ diverges from the optimal value.

The simple Encoding problem above is particularly helpful because if a solution weight vector exists, there can only be one vector in weight space that solves the problem exactly (assuming $t^{i=1} < t_1^o < t^{i=2} < t_2^o$). For example, the optimal value for the first weight can be obtained by replacing t in Equation 1 with the first desired spike time and solving for $w_{i=1}$. By measuring the distance of this weight to its optimal value throughout 1000 epochs of learning, we find that a critical parameter for learning interference is the distance between the two output spikes (Figure 3). Here, we observe three different long-term effects of learning interference: (1) weight fluctuating around the optimal value, (2) weight converges, but requires five to ten times more training iterations, and (3) weight diverges from the optimal value. We train the neuron using the PSD method (Yu et al., 2013), and initial weights are set to zero. This result suggests that even with two out-

put spikes, learning interference can either slow down convergence or prevent it altogether.

2.4. DTA Algorithm

In this section, we describe the DTA algorithm for training SNNs. We first formulate the algorithm to solve the Encoding task, then describe the (minimal) changes required to solve the Decoding task. During learning, the network is trained for a number of epochs. Each epoch is divided into P training iterations. At each iteration we train the network using one input pattern which is chosen randomly without replacement from the dataset, so an epoch is finished when all input patterns have been presented once. Learning stops if the maximum number of epochs is reached, or the network responds to all input patterns correctly. In the Decoding task, this means responding to each pattern with the correct number of spikes. In the Encoding task, each output spike response to an input should on average be within $T = 1$ millisecond from a desired spike (see Appendix A for more detail).

2.4.1. Solving the Encoding Task

We now describe an iteration of the DTA algorithm for solving the Encoding task. The general idea of the algorithm is to convert the weight adjustment calculations into a linear constraint satisfaction problem. Optimising this satisfaction problem involves calculating a ratio of weight adjustments at all desired and actual spike times, with which all threshold constraints are simultaneously satisfied. Thus, in one DTA iteration we will calculate a large number of positive and negative weight adjustments (as in Equation 4) without having to simulate the neuron multiple times, which greatly improves computational efficiency.

More formally, we begin the learning iteration with weights w , and we will calculate weight adjustment Δw such that the membrane potential obtained using solution weights $w^* = w + \Delta w$ satisfies all threshold constraints. We replace the parameter η in Equation 4 with (unknown) variables specific to each output spike time. This means at time $t_a^d \in y_p$ the weight adjustment is multiplied by variable η_a^d , and at time $t_b^o \in o(\vartheta, \mathbf{x}_p, w)$ the adjustment is multiplied by variable η_b^o . This yields the DTA update equation for a channel i :

$$\Delta w_i = \sum_{a=1}^{|y_p|} \eta_a^d \sum_{t^i \in x_i} \kappa(t_a^d - t^i) + \sum_{b=1}^{|o(\vartheta, \mathbf{x}_p, w)|} \eta_b^o \sum_{t^i \in x_i} \kappa(t_b^o - t^i) \quad (8)$$

We calculate appropriate values for η_a^d and η_b^o by solving a constraint optimisation problem. We first note that in the SRM model it is well established that the reset function can be moved from $V(t)$ to ϑ without changing the computation of the neuron (Gerstner and Kistler, 2002). This means instead of resetting the membrane potential we increase the threshold at each spike time:

$$\begin{aligned} V_0(t) &= \sum_{i=1}^N w_i^* \sum_{t^i \in x_i} \lambda(t - t^i) \\ \theta(t) &= \vartheta + \vartheta \sum_{t^d \in y} \gamma(t - t^d) \end{aligned} \tag{9}$$

In this format, the membrane potential can be efficiently calculated using matrix multiplication, which simplifies computation for the optimisation step. The optimisation problem consists of the following linear constraints:

$$\begin{aligned} \theta(t) &= V_0(t), t \in y \\ \theta(t) &> V_0(t), t \in o(\vartheta, \mathbf{x}_p, w) \end{aligned} \tag{10}$$

Additionally, we impose the following domain constraints:

$$\begin{aligned} lb^d &\leq \eta_a^d \leq ub^d \\ lb^o &\leq \eta_b^o \leq ub^o \end{aligned} \tag{11}$$

These domains are necessary to constrain the sizes and directions ($lb^d > 0$ and $ub^o < 0$) of weight adjustments. The size constraint is necessary to minimise membrane potential overshoot, in which the threshold equality constraint is satisfied while $V_0(t)$ is decreasing, rather than increasing. The learning problem now reduces to an optimisation task, which can be solved with standard approaches. In our implementation, we use the Tulip linear optimiser Tanneau et al. (2021) which implements the interior-point method (Wright, 2005). Solution weights w^* is used as initial weights for the next iteration, if convergence is not yet reached.

It is important to also address the non-ideal situation wherein the above optimisation problem returns no feasible solutions. In this scenario, we set all η_a^d to a hyper-parameter $\eta = 0.001$, and all η_b^o to $-\eta$. It follows that the learning iteration where this happens is affected by learning interference, and thus the resulting output spikes may not be at desired timings. However, we find this approach works

very well, because the additional threshold inequality constraints allows the problem to become feasible in subsequent learning iterations, and so facilitating an exact solution. This is of course not a problem if a sub-sample of time points are used to impose additional threshold inequalities, however this may significantly increase the dimensionality of the optimisation problem.

Algorithm 1: DTA Algorithm for training output neurons in Encoding task

Data: $\mathbf{X} = \{\mathbf{x}_1, \mathbf{x}_2, \dots, \mathbf{x}_p\}$, $\mathbf{Y} = \{y_1, y_2, \dots, y_p\}$
 initialise neuron with weights w ;
 $accuracy \leftarrow 0.0$;
while $epoch < maxEpoch$ or $accuracy < 1.0$ **do**
 shuffle \mathbf{X} ;
 foreach \mathbf{x}_p in \mathbf{X} **do**
 compute $o(\vartheta, \mathbf{x}_p, w)$;
 compute Δw (Equations 8 & 10);
 $w^* \leftarrow w + \Delta w$;
 $w \leftarrow w^*$;
 end
 $accuracy \leftarrow \frac{\sum_{p=1}^P \Theta(vRD^*(T, \Delta t) - vRD(o(\vartheta, \mathbf{x}_p, w), y_p))}{P}$ (Appendix A);
end

2.4.2. Solving the Decoding Task

We now describe an iteration of the DTA algorithm for solving the Decoding task. The general idea is to first find appropriate desired spike timings for an input pattern, then calculate weight adjustments as in the previous section. The appropriate spike timings are chosen using a ‘dynamic threshold’ procedure, which is inspired by and adapted from Tempotron learning (Gütig and Sompolinsky, 2006; Gutig, 2016). The procedure is as follows: to generate an additional output spike, we lower the spiking threshold to some value $\vartheta^* < \vartheta$, such that the neuron generates one additional spike. Similarly, to elicit one fewer spike, we raise the threshold to $\vartheta^* > \vartheta$. We then simulate the neuron with ϑ^* to obtain a new set of output spike times $o(\vartheta^*, \mathbf{x}_p, w)$, which is used as desired output spike timings. The learning problem now reduces to an Encoding task. This dynamic threshold procedure is illustrated in Figure 4.

More formally, we begin the learning iteration by first simulating the neuron to obtain $o(\vartheta, \mathbf{x}_p, w)$. If the number of output spikes $|o(\vartheta, \mathbf{x}_p, w)|$ is different to the integer label l_p , we calculate an appropriate threshold ϑ^* . We obtain ϑ^* by

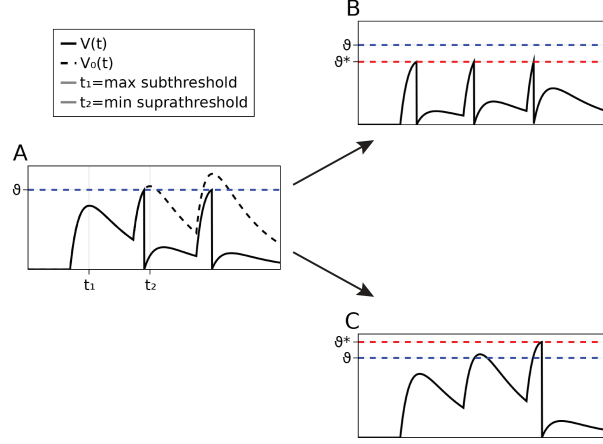


Figure 4: Dynamic threshold procedure for determining desired spike timings in Decoding tasks. **A:** Membrane potential $V(t)$ (solid line) and membrane potential without reset $V_0(t)$ (dashed line) of a neuron with two output spikes. The appropriate time to generate a new spike is t_1 , since $V(t_1)$ is closest to ϑ , thus requires the smallest weight adjustment. Similarly, t_2 is the appropriate time to remove an existing spike. **B:** decreasing threshold yields an extra spike at t_1 . **C:** increasing threshold removes the spike at t_2 . We use spike timings in B (3 spikes) and C (1 spike) as desired spike timings, then calculate weight adjustment as with the Encoding task.

interval halving in the interval $(0, 10\vartheta)$, stopping on the following conditions:

- $|o(\vartheta^*, \mathbf{x}_p, w)| = |o(\vartheta, \mathbf{x}_p, w)| + 1$ if we want more spikes
- $|o(\vartheta^*, \mathbf{x}_p, w)| = |o(\vartheta, \mathbf{x}_p, w)| - 1$ if we want fewer spikes

The output spike times $o(\vartheta^*, \mathbf{x}_p, w)$ is then chosen as desired spike times for \mathbf{x}_p . The problem now reduces to an Encoding task, and weight adjustment is

calculated as described in the previous section.

Algorithm 2: DTA Algorithm for training output neurons for Decoding task

Data: $\mathbf{X} = \{\mathbf{x}_1, \mathbf{x}_2, \dots, \mathbf{x}_p\}$, $\mathbf{Y} = \{l_1, l_2, \dots, l_p\}$
 initialise neuron with weights w ;
 $accuracy \leftarrow 0.0$;
while $epoch < maxEpoch$ **or** $accuracy < 1.0$ **do**
 shuffle \mathbf{X} ;
 foreach $\mathbf{x}_p \in \mathbf{X}$ **do**
 compute $o(\vartheta, \mathbf{x}_p, w)$;
 if $|o(\vartheta, \mathbf{x}_p, w)| < l_p$ **then**
 compute ϑ^* such that $|o(\vartheta^*, \mathbf{x}_p, w)| = |o(\vartheta, \mathbf{x}_p, w)| + 1$;
 else if $|o(\vartheta, \mathbf{x}_p, w)| > l_p$ **then**
 compute ϑ^* such that $|o(\vartheta^*, \mathbf{x}_p, w)| = |o(\vartheta, \mathbf{x}_p, w)| - 1$;
 $y_p \leftarrow o(\vartheta^*, \mathbf{x}_p, w)$;
 compute Δw (Equations 8 & 10);
 $w^* \leftarrow w + \Delta w$;
 $w \leftarrow w^*$;
 end
 $accuracy \leftarrow \frac{\sum_{\mathbf{x}_p \in \mathbf{X}} \delta(|o(\vartheta, \mathbf{x}_p, w)| - l_p)}{P}$
end

2.5. Memory Capacity

In this section, we evaluate the capacity of the DTA algorithm to memorise (fit) training data. All benchmarks presented here measure the capacity of single spiking neurons. All input patterns for training are randomly generated as described in Section 2.1. During training, the order of pattern presentation as well as initial weights are controlled across all methods being compared.

2.5.1. Capacity in the Encoding Task

We first investigate the memory capacity of the DTA algorithm in the Encoding task, compared to existing algorithms in the literature. For random input and output spike sequences, Memmesheimer et al. (2014) has defined memory capacity as the maximal length of inputs T_α that a single spiking neuron can learn. They approximate that this quantity is given by:

$$T_\alpha \approx \frac{N\sqrt{\tau_m\tau_s}}{\frac{-2\nu_{\text{out}}\sqrt{\tau_m\tau_s}}{1+\nu_{\text{out}}\sqrt{\tau_m\tau_s}}\log\left(\frac{\nu_{\text{out}}\sqrt{\tau_m\tau_s}}{1+\nu_{\text{out}}\sqrt{\tau_m\tau_s}}\right)} \quad (12)$$

Here, ν_{out} is the output spiking rate, and N is the number of input channels. We will show that the DTA algorithm is able to achieve this maximal memory capacity within 100 epochs of learning. In addition, Memmesheimer et al. (2014) also showed that the memory capacity should be the same for learning multiple short input patterns, and for learning a single long input pattern. For completeness, we will evaluate our algorithm when learning short and long input patterns. In simulations, we compare the performance of our algorithm with the PSD algorithm (Yu et al., 2013), the FILT algorithm (Gardner and Grüning, 2016), and the ReSuMe algorithm (Ponulak and Kasiński, 2010). These existing algorithms all share the following weight update equation:

$$\Delta w_i = \sum_{a=1}^{|y_p|} \eta \sum_{t^i \in x_i} \kappa(t_a^d - t^i) + \sum_{b=1}^{|o(\vartheta, \mathbf{x}_p, w)|} \eta \sum_{t^i \in x_i} \kappa(t_b^o - t^i)$$

In particular, the PSD uses $\kappa_{\text{PSP}}(t)$, FILT uses $\kappa_{\text{FILT}}(t)$, and we implement a version of the ReSuMe algorithm which uses $\kappa_{\text{STDP}}(t)$. The similarity of this update equation with Equation 8 means that any differences between these algorithms and our DTA method is a direct result of our constraint optimisation formulation. As such, this allows us to demonstrate the performance improvements that is gained from addressing learning interference.

Our experimental setup is as follows: In the short input scenario, the neuron is trained to memorise short input patterns of length $T = 400$. The experiment is repeated over 50 independent trials. In each trial, we begin by training the neuron with only one input pattern. We then subsequently and iteratively increase the number of input patterns, such that the neuron learns two input patterns, then three, and so on. The experiment concludes at the point where half of all experimental trials failed to converge within 500 training epochs, then we calculate T_α as the sum duration of all input patterns. In the long input scenario, the neuron is trained to memorise only a single long input pattern of variable length T . In each independent trial, we begin by training the neuron with an input of duration $T = 1000$. We then iteratively increase T by increments of 100. The experiment concludes when half of all experimental trials have converged, and T is taken as T_α . All algorithms are trained with learning rate hyper-parameter $\eta = 0.01$.

Learning Scenario	Method	T_α
	Theoretical Bound (Equation 12)	17200
Multiple Short Patterns	DTA- κ_{STDP}	9000
	DTA- κ_{PSP}	18100
	DTA- κ_{FILT}	6000
	ReSuMe- κ_{STDP}	7500
	PSP	5400
	FILT	13000
Single Long Pattern	DTA- κ_{STDP}	15000
	DTA- κ_{PSP}	17300
	DTA- κ_{FILT}	6200
	ReSuMe- κ_{STDP}	10900
	PSP	7000
	FILT	4800

Table 1: Maximal memory capacity measurements in the Encoding task, when learning to memorise multiple short input patterns or learning a single long input pattern. The experimental parameters are $N = 500$, $\nu_{\text{in}} = \nu_{\text{out}} = 0.005$, $\tau_m = 20$, $\tau_s = 5$. In both learning scenarios, DTA- κ_{PSP} reaches the theoretical upper bound estimated by Memmesheimer et al. (2014). We note that standard deviations are not reported in this table, because each data point already represents 50 independent trials.

By substituting our parameter values into Equation 12, the theoretical maximal memory capacity evaluates to $T_\alpha \approx 17200$. Table 1 shows that our algorithm achieves this capacity when κ_{PSP} is used as the kernel function. Notably, our algorithm achieves this desired performance in both learning scenarios, whereas the ReSuMe, PSD, and FILT algorithms all achieve low capacity ($T_\alpha < 10000$) with at least one scenario. To the best of our knowledge, the only other learning algorithms which are capable of reaching this memory capacity are the FP and HTP algorithms (Memmesheimer et al., 2014), and they require fifty million epochs for convergence in their benchmarks.

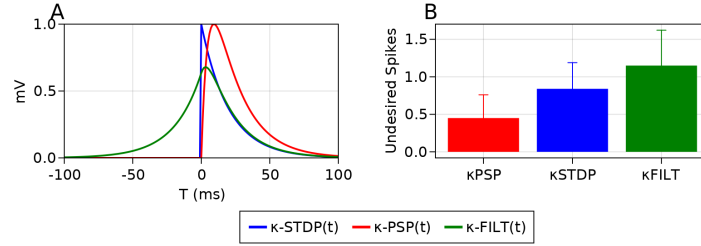


Figure 5: **A:** The shapes of the kernel functions $\kappa(t)$ used in this work. **B:** Average number of additional threshold inequality violations (output spikes not at desired timings) after a random number of learning iterations (between 1 and 10) of learning a single input pattern with five desired output spikes, repeated over 5000 independent trials. Error bars are standard deviations.

Regarding the reduced performance of our algorithm when using κ_{STDP} and κ_{FILT} as the learning window, we find that these functions cause much more frequent occurrences of threshold inequality violations during learning. This means that after a learning iteration, we observe undesired output spikes which do not occur within one millisecond of a desired spike timing (data shown in Figure 5B). There must then be a property of the κ_{STDP} and κ_{FILT} kernels which results in this undesired behaviour. The most evident characteristic which separates these kernels from κ_{PSP} is their *anti-causal* property. With κ_{PSP} weights are always adjusted proportionately to their membrane potential contribution; however, with κ_{STDP} and κ_{FILT} weights which do not contribute at all at a desired spike time may be given disproportionately large adjustment. We suspect this causes additional threshold inequality violations at temporally uncorrelated timings.

2.5.2. Capacity in the Decoding Task

We now investigate the memory capacity of the DTA algorithm in the Decoding task, compared to existing algorithms in the literature. Here, we define the

memory capacity as the number of different input patterns that a neuron can learn, denoted as P_α . In this task, the neuron has to discriminate input patterns into five classes, labelled 1 to 5. The experiment is repeated over 50 independent trials. In each trial, each class initially contains only one input pattern. We then evenly and iteratively increase the number of input patterns, such that each class has two patterns, then three, and so on. We stop adding input patterns when half of all trials have failed to converge within 100 epochs, and the experiment concludes at this point. All input patterns are generated with $N = 500$ channels, duration $T = 50$, and spiking rate $\nu_{\text{in}} = 0.005$.

We compare our algorithm with the MST (Gutig, 2016) and the EMLC (Li and Yu, 2020) algorithms, which are both state-of-the-art methods for Decoding. These algorithms are trained with learning rate $\eta = 0.01$, with no momentum acceleration. Simulation results are shown in Table 2. Overall, our algorithm achieves approximately twice the maximal memory capacity when compared to the EMLC algorithm, and three times compared to the MST algorithm.

Table 2: Comparison of memory capacity in the Decoding task, when each method is limited to 100 training epochs. Each data point is measured as the point where 50% of all trials failed to converge.

Method	Memory Capacity
MST (Gutig, 2016)	110
EMLC (Li and Yu, 2020)	165
DTA- κ_{PSP}	355

The improved performance of our method in the Decoding task may appear unusual, because here exact spike timings do not matter and learning interference is only relevant when weight adjustment causes existing spikes to erroneously disappear. To better explain our result, we investigate the difference in complexity scaling of our algorithm compared to the EMLC algorithm. Importantly, we find that our algorithm achieves better complexity scaling with respect to the spiking threshold ϑ . Figure 6 shows that our algorithm exhibits constant scaling, whereas the EMLC algorithm scales linearly. This result is intuitive, as while our algorithm changes the number of output spikes by one each iteration, whereas the EMLC algorithm requires a number of iterations to do this (as a linear function of ϑ/η). This means that in addition to mitigating effects of learning interference, our treatment of ‘dynamic’ learning rate variables also play an important role in the improved efficiency of our method.

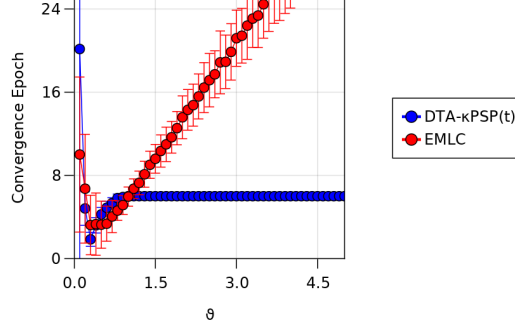


Figure 6: Time complexity scaling of the DTA method compared with the EMLC method (Li and Yu, 2020), with respect to the spiking threshold ϑ .

2.5.3. Multi-Spike Decoding Capacity of SRM Neuron

The improved efficiency of our method presents an opportunity to investigate the Decoding capacity of spiking neurons in further detail. The capacity benchmark task presented in the previous section (with a small number of classes) is common in the literature (Miao et al., 2018; Xiao et al., 2019; Li and Yu, 2020), however we now introduce a slightly different definition of capacity, denoted as C_α . We define C_α as the maximal number of classes that a neuron can learn in the Decoding task, where each class only has a single input pattern. We constrain the class labels to fill the integer range from 1 to C_α . This capacity can be interpreted as the ability of the neuron to simultaneously satisfy different output requirements, while the input statistics (input spiking rate) remains constant for all classes. Generally, we are interested in the experimental conditions that maximises C_α .

We will measure C_α as follows. In each trial, the neuron initially learns only one class, then we subsequently and iteratively increase the number of classes, such that the neuron learns two, then three classes, and so on. The experiment concludes at the point where 50% of all independent trials have failed to converge within 100 epochs. Due to the very large computational requirements of this experimental setup, we only train the neuron using the DTA algorithm.

Importantly, in the large N limit ($N > 10000$) we find that C_α can be expressed as a function of a parameter $\nu_{\text{in}}\tau$, where ν_{in} is the input spiking rate, and $\tau = \sqrt{\tau_m\tau_s}$ is called the PSP correlation time. Specifically, C_α decreases with increasing $\nu_{\text{in}}\tau$ (Figure 7A). Assuming ν_{in} is fixed, τ should then be small in order to maximise the capacity. This means that the neural dynamics that maximises

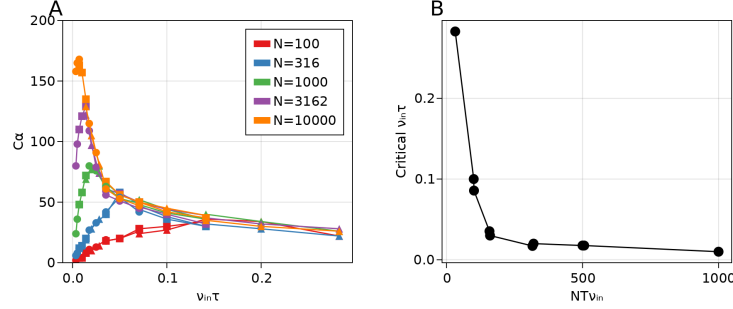


Figure 7: **A:** Decoding capacity C_α , plotted against $\nu_{in}\tau$ where ν_{in} is the input spike rate and τ is the PSP correlation time. In general, C_α can be expressed as an exponentially decaying function of $\nu_{in}\tau$. Symbols (circle, square, triangle) respectively represent different series measured with $\tau_m = 10, 20, 40$. **B:** the critical values of $\nu_{in}\tau$ at which the capacity deviates from the behaviour described in A, plotted against the average number of spikes in an input pattern. Each data point represents 50 independent trials.

C_α in the large N limit is such that the membrane potential is able to rise rapidly upon receiving an input spike, and also decays rapidly afterwards. The neuron then operates in a fashion which is reminiscent of coincidence-detection, where each output spike is only generated by coincident inputs during a very small time window. Outside of the large N limit, the capacity quickly deviates from the behaviour described above. More specifically, for $\nu_{in}\tau$ smaller than a critical value, C_α instead increases with increasing $\nu_{in}\tau$. We find that the critical value depends only on the average number of spikes in an input pattern (calculated as $NT\nu_{in}$), as shown in Figure 7B.

The above result is consistent with the conclusions published in Memmesheimer et al. (2014) for the Encoding task, and in Rubin et al. (2010) for the binary (two-class) Decoding task. In both of these studies, the memory capacity decreases as τ increases, assuming that N is large. This then suggests that regardless of the specific learning task, or indeed regardless of whether learning is single-spike or multi-spike, the ability for the membrane potential to rapidly respond to new inputs or forget past inputs is central to the computational capacity of spiking neuron models.

2.6. Practical Learning Tasks

In this section, we evaluate the ability of our algorithm to generalise from training data to unseen examples. We will apply our algorithm to the IRIS dataset (Anderson, 1936; Fisher, 1936) and the MNIST dataset (LeCun and Cortes, 2010),

formulating both experiments as Decoding classification tasks using multiple spikes.

2.6.1. IRIS Dataset

Here, we evaluate the generalisation ability of our algorithm on the IRIS dataset, compared to the EMLC (Li and Yu, 2020) and MST (Gutig, 2016) algorithms, which are both state-of-the-art Decoding methods. The IRIS dataset consists of 150 samples evenly divided into three classes of different species of the *iris* plant, two classes of which are not linearly separable. Each sample consists of four continuous and real-valued features: petal width, petal length, sepal width, and sepal length. To encode the features into spike times, we use population encoding (Bohte et al., 2002) with Gaussian receptive fields of the form $G(v, \mu_j, \sigma) = \exp(-(x - \mu_j)^2/2\sigma^2)$, wherein v is the feature value. Each feature is represented by $M = 10$ identically shaped Gaussian functions centered at:

$$\mu_j = I_j^{\min} + \left(\frac{2i-3}{2}\right) \left(\frac{I_j^{\max} - I_j^{\min}}{M-2}\right), j \in \{1, 2, \dots, M\}$$

Here, I_j^{\max} and I_j^{\min} represents the maximum and minimum of the j -th feature, respectively. The spread of the Gaussian functions are determined by:

$$\sigma = \frac{1}{\beta} (I_j^{\max} - I_j^{\min}) (M-2)$$

Here, $1 \leq \beta \leq 2$ is an adjustment factor, which is set to 1.5 because this value produced the best classification results. As such, each feature value v is converted into M output values $0 \leq G(v, \mu_j, \sigma) \leq 1$, which is then converted into spike times as $t_j = T - G(v, \mu_j, \sigma)T$. In simulation, we choose $T = 10$ as this value was determined to provide the best results.

For learning, we use a SNN with one input layer and one trainable output layer containing three output neurons. Each output neuron is trained to respond to one (target) class of inputs with $s = 10$ output spikes, and to remain quiescent for the other two (null classes). A grid-based parameter search showed that generalisation accuracy improves as s increases, but does not improve for $s > 10$. Finally, a Winner-Take-All output encoding scheme is applied to the output layer, in which the prediction is represented by the neuron with the most number of spikes. Since our network implements no lateral inhibition between output neurons, the WTA scheme helps improve prediction accuracy on difficult or partially-learned input patterns, for example when a neuron does not generate precisely s spikes for target patterns or does not remain completely quiescent for null patterns Li and Yu

(2020). We note also that in any training iteration, if the network prediction is correct *because* of the WTA scheme, weight adjustments are still made to any output neurons with an incorrect number of output spikes (as in the previous example).

The networks are trained for 20 epochs. During each trial, the input patterns are randomly divided into a training set (50% of patterns) and a testing set (50% of patterns) for cross-validation. Similarly to the previous section, in each trial we control the order of pattern presentation and the initial weights of the network. Simulation results for 50 independent trials are presented in Table 3. In terms of performance, the DTA algorithm achieves approximately 7% better training accuracy, and approximately 10% better generalisation accuracy compared to EMLC and MST. In terms of convergence speed, the DTA method also demonstrates an improvement. To achieve the same level of generalisation accuracy that the DTA method achieves after one epoch of training, the EMLC and MST methods both require approximately seven epochs. After the first four training epochs, the DTA method achieves better performance than the final accuracy demonstrated by the EMLC or MST algorithms (Figure 8).

Table 3: Training and test accuracy of the proposed method on the IRIS flower dataset formulated as a Decoding problem.

Method	Train (%)	Test (%)
DTA- κ_{PSP}	96.8 ± 2.03	96.1 ± 2.61
EMLC (Li and Yu, 2020)	89.6 ± 6.91	84.8 ± 6.10
MST Gutig (2016)	89.4 ± 2.62	86.3 ± 4.98

The Friedman test was used on the test data, to determine whether or not there is a significant difference between the average ranks of the three algorithms in Table 3 under the null hypothesis. The calculated Q -statistic is $Q = 16.8$, which yields a corresponding p -value of $p = 0.0002$. Thus, we reject the null hypothesis that the three algorithms have no significant differences in generalisation accuracy. The Nemenyi test was used for post-hoc analysis to determine pairwise differences, which reported significant differences between the DTA method, when compared to the EMLC and MST methods (both yielding p -values of 0.001). When comparing the EMLC and MST methods, the statistical difference was not significant ($p = 0.425$).

Notably, in this classification task our single-layer network performance is comparable to multi-layer approaches in the literature. In particular, we achieve similar predictive accuracy when compared to Bohte et al. (2002) (reported 96.1%), Sporea and Grüning (2013) (94%), and Gardner and Grüning (2021) (95.2%). The

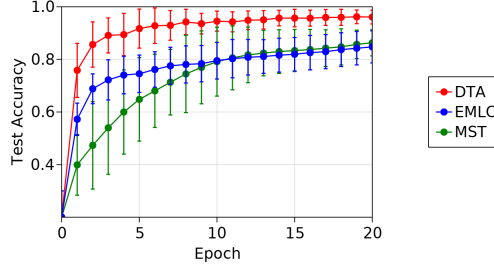


Figure 8: Generalisation accuracy on the IRIS dataset, over 20 epochs of training. Error bars are standard deviations. Each data point represents 50 independent trials.

works noted here all utilise a multi-layer architecture with one hidden layer, containing 9-10 hidden neurons. In addition, Bohte et al. (2002) and Gardner and Grüning (2021) uses $M = 12$ population input neurons to encode each feature, which is more than our $M = 10$. In terms of convergence speed, our method demonstrates an improvement compared to existing methods. For example, Gardner and Grüning (2021); Tavanaei and Maida (2019); Taherkhani et al. (2018) reported high ($> 94\%$) predictive accuracies after 30, 120, and 100 training epochs, respectively. Our setup reaches this performance after the first 8 epochs on average. It is also important to note that while some of the works discussed here also performs classification with multiple output spikes, none of them utilise a Decoding classification scheme, which may also be a factor in the improved accuracy and learning speed which we observe in our results.

2.6.2. MNIST Dataset

In this section, we compare the generalisation accuracy of our algorithm with the EMLC algorithm (Li and Yu, 2020), the MST algorithm (Gutig, 2016), and traditional gradient-descent using back-propagation. The MNIST dataset consists of images with size 28×28 pixels, split into ten classes labelled from 0 to 9 (LeCun and Cortes, 2010). Since the spiking algorithms that we will test are all limited to one trainable layer, we will preprocess the data using a hybrid ANN-SNN framework called CSNN (Xu et al., 2018), and only train the (spiking) output layer. In this way, we only test the capabilities of these algorithms to distinguish input patterns, not feature extraction.

The CSNN framework combines traditional CNN with a SNN classifier. More formally, the architecture has two layers of rate-coded neurons, and two layers of spiking neurons. Computation through the network can be decomposed into three parts: feature extraction, temporal encoding, and classification. The technical

details of this architecture are as follows:

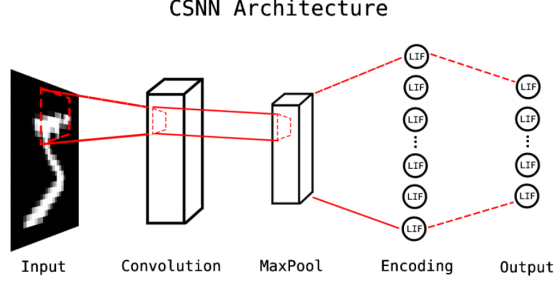


Figure 9: Overview of the CSNN architecture (Xu et al., 2018). The Convolution and MaxPool layers are composed of rate-coded neurons, while the Encoding and Output layers are composed of spiking neurons. In our setup, the Encoding layer has 864 neurons and the Output layer has 10 neurons.

First, we train a traditional rate-coded CNN, which provides feature extraction capabilities. The CNN only has three layers: a convolutional layer (6C5), a max-pooling layer (2P2), and a fully connected output layer with 10 neurons. We train this CNN using traditional back-propagation with cross-entropy error function for 30 epochs, then the CNN parameters are fixed and the output layer discarded. The resulting partial-CNN model (the convolutional and pooling layer) performs extraction of invariant local feature maps from the input image.

The feature maps produced by the above partial-CNN must be converted into a spike-based encoding. To this end, the real-valued activations of the pooling layer are linearly mapped to spike times in a time window of length $T = 50$. The pooling layer feature maps are flattened to a vector of 864 activation values. We denote the i -th activation value A_i and the corresponding spike time t_i^{spike} . Encoded spike times are calculated as $t_i^{\text{spike}} = T - T \cdot A_i$. These timings are then used as spike times for the encoding layer of LIF neurons. Additionally, any encoding neurons with spike time $t_i^{\text{spike}} = T$ (corresponds to $A_i = 0$) do not spike, as their activation is considered too low to induce input spikes.

The encoding layer is fully connected to the output layer, which consists of ten spiking neurons which will be trained. Similarly to the previous section, each neuron is responsible for responding to a ‘target’ class with $s = 10$ output spikes, remaining quiescent for all other classes, and a WTA scheme is applied to the output layer. All spiking neurons are initialised with $\tau_m = 20.0$ and $\tau_s = 5.0$, with initial weights drawn from a Gaussian distribution with mean 0.01 and standard deviation 0.01.

To evaluate learning performance, we use the full MNIST data of 60000 train and 10000 test images. We train the CSNN described above using the DTA method (CSNN-DTA), the EMLC method (CSNN-EMLC), and the MST method (CSNN-MST). All networks are trained for 20 epochs, with learning rate $\eta = 0.001$, without momentum acceleration or learning rate adaptation. As with the previous sections, order of pattern presentation and initial weights are controlled to be the same for all methods in each trial. Simulation results for 10 independent trials comparing these three methods are shown in Table 4.

Overall, the DTA method outperforms the EMLC and MST methods in both accuracy and convergence speed. Regarding the generalisation performance, the DTA method achieves approximately 5% better accuracy compared to EMLC, and approximately 10% better compared to MST. For good generalisation performance, it is often useful to consider early-stopping in order to prevent over-fitting to training data. If we consider a suitable early-stopping point to be within 1% of the final accuracies reported in Table 4, then the DTA method only requires approximately six training epochs, the EMLC method requires ten epochs, and the MST method requires 18 epochs. This means that the DTA method reaches convergence faster than compared to the EMLC or MST. Similarly, convergence to a good ($> 90\%$) solution is achieved by the DTA method in just 1 epoch, compared to 7 epochs for the EMLC method. The MST method does not achieve this accuracy after 20 epochs of training (Figure 10).

Method	Train accuracy (%)	Test accuracy (%)
CSNN-DTA	97.57 ± 0.82	97.54 ± 0.44
CSNN-EMLC (Li and Yu, 2020)	94.15 ± 0.26	92.27 ± 0.26
CSNN-MST (Gutig, 2016)	89.98 ± 4.61	86.91 ± 4.26

Table 4: Performance comparison of CSNN trained with the MST, EMLC, and DTA methods on the MNIST dataset. Each data point is averaged over 10 independent trials.

The Friedman test was used here to determine whether or not there is a significant difference between the average ranks of the three algorithms in Table 4 under the null hypothesis. The calculated Friedman statistic is $F_F = 47.25$. With three treatments (methods) and 10 independent trials, F_F is distributed according to the F -distribution with 3 and 18 degrees of freedom, which for 5% significant level yields the critical value of 3.16. Since F_F is greater than the critical value, the null hypothesis can be rejected and the differences between the three methods is considered significant. The Nemenyi test was used for post-hoc analysis, which reported significant differences in the predictive performance between the DTA

and EMLC methods (with p -value of 0.0199), and between the DTA and MST methods (with p -value of 0.001). These results indicate that the DTA method demonstrate statistically significant improvement in generalisation performance compared to EMLC and MST. Additionally, we note that even though the CSNN architecture was fundamentally similar, we did not compare our results with those of Xu et al. (2018), because they did not train output neurons to fire multiple spikes.

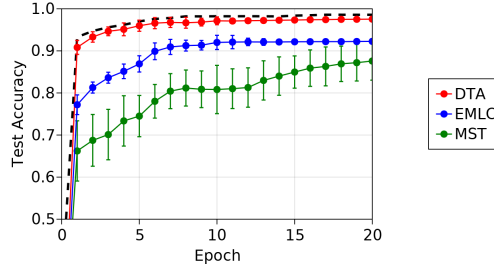


Figure 10: Generalisation accuracy on the MNIST dataset, over 20 epochs of training. Error bars are standard deviations. Each data point represents 10 independent trials. Black dashed lines represents average accuracy of a traditional rate-coded convolutional neural network with the convolution and pooling weights fixed to the same weights which are used in the CSNN.

In addition to comparing the DTA method with other spike-based approaches, we also obtained results from a traditional non-spiking CNN (dashed line in Figure 10). This CNN has one convolution and one pooling layer, the weights of these layers are initialised to be the same as those layers of the CSNN, and kept fixed throughout learning. The pooling layer is fully connected to an output layer of 10 rate-coded sigmoidal neurons, and we train this output layer weights with gradient-descent with cross-entropy loss. A small (maximum 0.1) amount of uniform noise is added to the CNN loss during training for regularisation. The order of pattern presentation is controlled to be the same as training the CSNN. This setup allows us to directly compare our spike-based method with the traditional ANN training approach. Overall, the DTA method demonstrates comparable generalisation accuracy as well as convergence speed to that of the CNN. After one epoch of training, CSNN-DTA is approximately 2% worse than the CNN, and this gradually improves to a final difference of 1% after 20 epochs. In comparison, EMLC and MST are approximately 6% and 11% worse than the CNN in terms of final accuracy. We found no statistically significant difference between DTA and the rate-coded CNN in terms of final generalisation performance ($p = 0.507$). These results suggest that our method is competitive with traditional ANN learn-

ing, even without any regularisation strategies.

3. Discussions & Further Work

In this paper, we present an efficient learning algorithm to address the problem of learning interference in multi-spike SNN classification problems. We show that training efficiency can improve significantly if interference is addressed. Learning interference has been previously acknowledged in the literature (Xu et al., 2013; Memmesheimer et al., 2014; Gardner and Grüning, 2016; Xie et al., 2016; Taherkhani et al., 2020) for both single-layer and multi-layer SNNs. It was suggested that ‘Bigger PSP, Bigger Adjustment’ (BPBA) principle can minimise learning interference (Xu et al., 2013; Luo et al., 2019; Zhang et al., 2021). However, we have shown that the PSD algorithm Yu et al. (2013) is affected by learning interference, even while adhering to the BPBA principle. Another suggested solution is the first-error approach presented by Memmesheimer et al. (2014), which successfully mitigates the effects of learning interference in Encoding tasks, at the cost of significantly lower learning efficiency. Other methods which are derived from the Widrow-Hoff rule (Widrow and Lehr, 1990; Ponulak, 2005; Florian, 2012; Yu et al., 2013; Gardner and Grüning, 2016) does not mitigate learning interference in their derivation, but instead they make modifications to empirical benchmark procedures (such as ensuring output spikes are far apart, or constraining input channels to only fire once).

We note that the linear constraints optimisation step of our algorithm bears similarities to the CONE method (Lee et al., 2016) for analytically calculating optimal solution weights. In particular, the CONE method also utilise threshold constraints to calculate weights. In addition, the CONE method requires additional objective functions which enforce the causality of weights leading to output spikes. In our algorithm, the kernel functions $\kappa(t)$ takes this role, which simplifies the computation to only linear constraints. The flexibility of the ‘causality’ parameters in the CONE method is maintained by simply choosing different $\kappa(t)$ in our method. The CONE method also has several limitations which do not affect our method: it is only applicable to discrete-time neurons, where the set of threshold inequalities are finite. Also, it is a batch method, which requires all the input and output data to be available at the start of training. This requirement is not always feasible, and computation with the CONE algorithm quickly becomes intractable for larger datasets (Lee et al., 2016). However, we note that with minor modifications to our algorithm, such as appropriate sub-sampling of the input pattern duration, our method can also be formulated as a batch method. This flexibility is

an important property for computational analysis, as batch algorithms are useful for quickly searching the solution space of a fixed-size problem.

The fundamental difficulty in extending the DTA method to multi-layer applications is in the use of the constraint satisfaction formulation. In a multi-layer SNN, the input spike timings arriving at the output layer from a hidden layer is not fixed, which means Equation 9 cannot be easily computed. There are two possible approaches to overcome this difficulty. The first approach is to apply a ‘spike jitter’ to output spike timings of hidden layers similar to Xie et al. (2016). This means the timing of each existing spike from a hidden layer neuron is simply shifted in the direction that minimises the difference between desired and actual output timings. Network training could then be carried out in a layer-wise fashion from the input layer to output layer, letting the shifted timings of one layer serve as the input timings for the following layer. The second approach is to consider each input spike t_i in Equation 9 as variables in the constraint satisfaction problem. Feasibility of the solutions then only depends on whether appropriate domain constraints can be determined for t_i . Out of these two approaches, we consider the former (spike jitter) to be more viable, as in the second approach the constraint satisfaction would no longer be linear, which increases the computational complexity of the problem greatly.

The central outcome of this work is that learning interference can be resolved by simultaneous weight adjustments in a global and temporally correlated manner. It is now important to consider this intuition from the gradient-descent perspective, as backpropagation remains highly relevant to training multi-layer networks (Tavanaei et al., 2019). With backpropagation, network weights are adjusted to minimise a differentiable error function \mathbb{E} . As an example, we can consider the error function suggested by (Xu et al., 2013):

$$\mathbb{E} = \frac{1}{2} \sum_{j=1}^{|y_p|} (t_j^d - t_j^o)^2 = \frac{1}{2} \sum_{j=1}^{|y_p|} \mathbb{E}_j$$

In the above equation, \mathbb{E} is formulated as a sum of different components \mathbb{E}_j , with each index j corresponding to a desired output spike time t_j^d . Derivation of the above equation will result in a learning rule which applies weight adjustments in a local and temporally uncorrelated fashion (as opposed to the above intuition). By this we mean that for some integer j , if $\mathbb{E}_j = 0$ then this component contributes nothing to the gradient because the j -th spike is already converged. In a similar manner to the first-error approach demonstrated in Figure 2, by minimising a different component $\mathbb{E}_{i \neq j} \neq 0$ we may increase \mathbb{E}_j . This means that in the

process of locally minimising each component, we may observe a net increase in \mathbb{E} , rather than the expected net decrease. This example of learning interference can be easily extended to other error functions in the literature such as (Lin et al., 2017; Taherkhani et al., 2018; Sporea and Grüning, 2013). This means that regardless of derivation, the learning interference problem exists at the level of the construction of the function \mathbb{E} . An analogy to the DTA method would now suggest that to maintain convergence of t_j^o in the above example, we should set \mathbb{E}_j to some non-zero value. The exact calculation of this value is still problematic, as this requires calculating the correlation of t_j^o with every other existing and desired timings. Notwithstanding, the significant efficiency improvements of our method in the single-layer SNN application suggests that resolving learning interference is also a worthwhile problem for designing more efficient multi-layer SNNs.

References

- Anderson, E. (1936). The species problem in iris. *Annals of the Missouri Botanical Garden*, 23(3):457–509.
- Bohte, S. M., Kok, J. N., and La Poutre, H. (2002). Error-backpropagation in temporally encoded networks of spiking neurons. *Neurocomputing*, 48(1-4):17–37.
- Booij, O. and tat Nguyen, H. (2005). A gradient descent rule for spiking neurons emitting multiple spikes. *Information Processing Letters*, 95(6):552–558.
- Borst, A. and Theunissen, F. E. (1999). Information theory and neural coding. *Nature neuroscience*, 2(11):947–957.
- Fisher, R. A. (1936). The use of multiple measurements in taxonomic problems. *Annals of eugenics*, 7(2):179–188.
- Florian, R. V. (2012). The chronotron: A neuron that learns to fire temporally precise spike patterns. *PloS one*, 7(8):e40233.
- Gardner, B. and Grüning, A. (2016). Supervised learning in spiking neural networks for precise temporal encoding. *PloS one*, 11(8):e0161335.
- Gardner, B. and Grüning, A. (2021). Supervised learning with first-to-spike decoding in multilayer spiking neural networks. *Frontiers in computational neuroscience*, 15:25.
- Gerstner, W. and Kistler, W. M. (2002). *Spiking Neuron Models Single Neurons, Populations, Plasticity*. Cambridge University Press.
- Ghosh-Dastidar, S. and Adeli, H. (2009). A new supervised learning algorithm for multiple spiking neural networks with application in epilepsy and seizure detection. *Neural networks*, 22(10):1419–1431.
- Gütig, R. and Sompolinsky, H. (2006). The tempotron: a neuron that learns spike timing–based decisions. *Nature Neuroscience*, 9:420–428.
- Gütig, R. (2014). To spike, or when to spike? *Current opinion in neurobiology*, 25:134–139.
- Gutig, R. (2016). Spiking neurons can discover predictive features by aggregate-label learning. *Science*, 351:aab4113–aab4113.

- LeCun, Y. and Cortes, C. (2010). MNIST handwritten digit database. <http://yann.lecun.com/exdb/mnist/>.
- Lee, W. W., Kukreja, S. L., and Thakor, N. V. (2016). Cone: Convex-optimized-synaptic efficacies for temporally precise spike mapping. *IEEE transactions on neural networks and learning systems*, 28(4):849–861.
- Li, S. and Yu, Q. (2020). New efficient multi-spike learning for fast processing and robust learning. *Proceedings of the AAAI Conference on Artificial Intelligence*, 34:4650–4657.
- Lin, X., Wang, X., and Hao, Z. (2017). Supervised learning in multilayer spiking neural networks with inner products of spike trains. *Neurocomputing*, 237:59–70.
- Luo, X., Qu, H., Zhang, Y., and Chen, Y. (2019). First error-based supervised learning algorithm for spiking neural networks. *Frontiers in Neuroscience*, 13.
- Maass, W. (1997). Networks of spiking neurons: The third generation of neural network models. *Neural Networks*, 10:1659–1671.
- Memmesheimer, R.-M., Rubin, R., Ölveczky, B. P., and Sompolinsky, H. (2014). Learning precisely timed spikes. *Neuron*, 82:925–938.
- Miao, Y., Tang, H., and Pan, G. (2018). A supervised multi-spike learning algorithm for spiking neural networks. *2018 International Joint Conference on Neural Networks (IJCNN)*.
- Mohammed, A., Schliebs, S., Matsuda, S., and Kasabov, N. (2012). Span: Spike pattern association neuron for learning spatio-temporal spike patterns. *International journal of neural systems*, 22(04):1250012.
- Ponulak, F. (2005). Resume-new supervised learning method for spiking neural networks [j]. *Institute of Control and Information Engineering, Poznan University of Technology*.
- Ponulak, F. and Kasiński, A. (2010). Supervised learning in spiking neural networks with resume: Sequence learning, classification, and spike shifting. *Neural Computation*, 22:467–510.

- Prieto, A., Prieto, B., Ortigosa, E. M., Ros, E., Pelayo, F., Ortega, J., and Rojas, I. (2016). Neural networks: An overview of early research, current frameworks and new challenges. *Neurocomputing*, 214:242–268.
- Rossum, M. v. (2001). A novel spike distance. *Neural computation*, 13(4):751–763.
- Rubin, R., Monasson, R., and Sompolinsky, H. (2010). Theory of spike timing-based neural classifiers. *Physical Review Letters*, 105.
- Satuvuori, E. and Kreuz, T. (2018). Which spike train distance is most suitable for distinguishing rate and temporal coding? *Journal of neuroscience methods*, 299:22–33.
- Sporea, I. and Grüning, A. (2013). Supervised learning in multilayer spiking neural networks. *Neural computation*, 25(2):473–509.
- Taherkhani, A., Belatreche, A., Li, Y., Cosma, G., Maguire, L. P., and McGinnity, T. M. (2020). A review of learning in biologically plausible spiking neural networks. *Neural Networks*, 122:253–272.
- Taherkhani, A., Belatreche, A., Li, Y., and Maguire, L. P. (2018). A supervised learning algorithm for learning precise timing of multiple spikes in multilayer spiking neural networks. *IEEE transactions on neural networks and learning systems*, 29(11):5394–5407.
- Tanneau, M., Anjos, M. F., and Lodi, A. (2021). Design and implementation of a modular interior-point solver for linear optimization. *Mathematical Programming Computation*.
- Tavanaei, A., Ghodrati, M., Kheradpisheh, S. R., Masquelier, T., and Maida, A. (2019). Deep learning in spiking neural networks. *Neural Networks*, 111:47–63.
- Tavanaei, A. and Maida, A. (2019). Bp-stdp: Approximating backpropagation using spike timing dependent plasticity. *Neurocomputing*, 330:39–47.
- Van Rullen, R. and Thorpe, S. J. (2001). Rate coding versus temporal order coding: what the retinal ganglion cells tell the visual cortex. *Neural computation*, 13(6):1255–1283.

- Widrow, B. and Lehr, M. A. (1990). 30 years of adaptive neural networks: perceptron, madaline, and backpropagation. *Proceedings of the IEEE*, 78(9):1415–1442.
- Wright, M. (2005). The interior-point revolution in optimization: history, recent developments, and lasting consequences. *Bulletin of the American mathematical society*, 42(1):39–56.
- Xiao, R., Yu, Q., Yan, R., and Tang, H. (2019). Fast and accurate classification with a multi-spike learning algorithm for spiking neurons. *Proceedings of the Twenty-Eighth International Joint Conference on Artificial Intelligence*, pages 1445–1451.
- Xie, X., Qu, H., Liu, G., Zhang, M., and Kurths, J. (2016). An efficient supervised training algorithm for multilayer spiking neural networks. *PloS one*, 11(4):e0150329.
- Xu, Q., Qi, Y., Yu, H., Shen, J., Tang, H., and Pan, G. (2018). Csnns: An augmented spiking based framework with perceptron-inception. *Proceedings of the Twenty-Seventh International Joint Conference on Artificial Intelligence*.
- Xu, Y., Zeng, X., Han, L., and Yang, J. (2013). A supervised multi-spike learning algorithm based on gradient descent for spiking neural networks. *Neural Networks*, 43:99–113.
- Yu, Q., Tang, H., Tan, K. C., and Li, H. (2013). Precise-spike-driven synaptic plasticity: Learning hetero-association of spatiotemporal spike patterns. *Plos one*, 8(11):e78318.
- Zhang, Y., Qu, H., Luo, X., Chen, Y., Wang, Y., Zhang, M., and Li, Z. (2021). A new recursive least squares-based learning algorithm for spiking neurons. *Neural Networks*, 138:110–125.

Appendix A. Spike Train Distance Metric

In this appendix, we describe the spike train distance metric used in Encoding tasks to quantify the difference between desired and actual output sequences. In this paper, we use the van Rossum distance (Rossum, 2001). This measure is denoted as $vRD(o(\vartheta, \mathbf{x}_p, w), y_p)$ for a particular input pattern and output sequence. This measure provides a positive distance between spike sequences, with $vRD(o(\vartheta, \mathbf{x}, w), y_p) = 0$ meaning the actual and desired sequences are identical (perfect convergence). Here, we describe vRD calculation, and how we choose the necessary parameters. The measure is calculated as:

$$vRD = \sqrt{\frac{1}{\tau_q} \int_{-\infty}^{\infty} \left[\sum_{t^d \in y} \kappa_{VD}(t - t^d) - \sum_{t^o \in o(\vartheta, \mathbf{x}, w)} \kappa_{VD}(t - t^o) \right]^2 dt}$$

$$\kappa_{VD}(t) = \exp\left(\frac{-t}{\tau_q}\right) \Theta(t)$$

Here, the kernel $\kappa_{VD}(t)$ is used to convert sequences of discrete spikes into continuous functions. τ_q is a parameter which sets the time scale sensitivity of the metric. Based on analyses presented in Rossum (2001); Satuvuori and Kreuz (2018), we set $\tau_q = 100$ which provides a good sensitivity to both short-term spike jitter and missing/additional spikes.

It is practically impossible to achieve perfect convergence, due to limitations of computer precision during learning. We must then choose a parameter to denote ‘sufficiently good’ convergence for simulations. We choose this parameter to be the average distance between each pair of actual and desired output spikes, denoted as Δt , and set $\Delta t = 1$ in this work. This means we consider an output sequence to be converged if each output spike is (on average) within 1 millisecond of their desired timing. This allows us to calculate a minimum distance value, denoted as $vRD^*(T, \Delta t)$. Generally, if $vRD(o(\vartheta, \mathbf{x}_p, w), y_p) < vRD^*(T, \Delta t)$ for all values of index p , then learning is converged.

To calculate $vRD^*(T, \Delta t)$, we perform a numerical benchmark to measure the average distance values while varying the distances between actual and desired spike sequences. We first generate 19000 ‘template’ spike sequences with varying duration $100 \leq T \leq 10000$. We then apply a Gaussian spike jitter to each template spike sequence with variance $1 \leq \sigma \leq 10$. The mean difference of template and jittered spike times for each spike sequence are calculated and taken as Δt . The

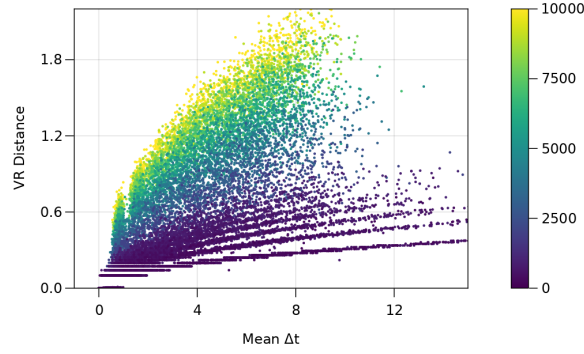


Figure A.11: Dependence of van Rossum distance values on the mean spike displacement (x-axis) and pattern duration T (colorbar) with filter time constant $\tau_q = 100$.

data is shown in Figure A.11. We then fit a Multiple Linear Regression model to the data, where the independent variables are T and Δt , which yields the following relation:

$$vRD^*(T, \Delta t) = 0.08\Delta t + 0.0001T$$

This function is used to calculate the minimum distance value with which we decide convergence. For example, an Encoding task with input patterns of duration $T = 1000$ requires the responses to each input pattern to be smaller than $vRD^*(T, \Delta t) = 0.18$.